Proc. 10th New Zealand Geothermal Workshop 1988

Heat Pipe Stability and Upstream Differencing

Mark McGuinness
Applied Mathematics Division, DSIR
Wellington, New Zealand

ABSTRACT

Questions raised at the previous Geothermal workshop about the stability of heat pipes are answered here. The instability found in numerical experiments on vapour-dominated and liquid-dominated heat pipes is here associated with the numerical procedure of upstream differencing.

INTRODUCTION

In the geothermal context a heat pipe is a porous medium in which heat is transferred vertically from depth with the steam rising and condensing at the top and liquid condensate falling to the bottom to boil again. This gravity driven counter-flow situation often has negligible net mass through-flow and is an important mechanism in vapour-dominated geothermal reservoir models (White et al, 1971; Straus and Schubert, 1981; Pruess, 1985; Truesdell and White, 1973.)

Numerical simulation of the heat pipe using the simulator MULKOM (Pruess, 1983) typically involves constructing a vertical stack of elements having a heat source or sink at one end which determines the heat flux Q and imposing a constant pressure and saturation boundary condition at the other end by placing a very large computational element there. In a paper at the previous geothermal workshop (McGuinness and Pruess, 1987) it was pointed out when numerically simulating a steady vapour-dominated heat pipe, it was necessary to have the constant pressure and saturation element at the bottom of the vertical numerical model. Conversely, if a steady liquid-dominated heat pipe was desired it was necessary to fix pressure and saturation at the top end. It has been found that this was a result of the numerical technique of upstream differencing. Before discussing this technique it is useful to review the steady state equations.

Steady State Conditions

The steady state conditions for zero net mass flux and a given heat flux Q through a 1-dimensional vertical heat pipe integrate to give (ignoring conduction)

$$u_v = -u_l = -u \qquad (1)$$

$$u h_{vl} = -Q \qquad (2)$$

where u_v, u_l are the Darcy velocities (mass flux densities kg/m^{2}s) for steam and liquid, h_{vl} is the latent heat of steam, and Q is the (negative) heat flux through the heat pipe.

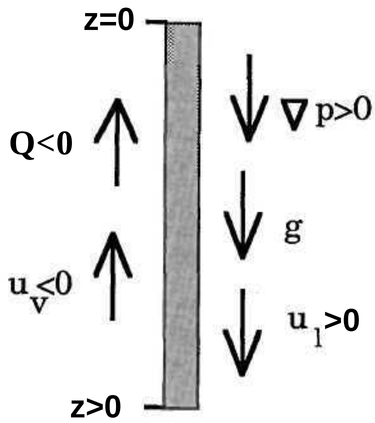

Figure 1. A ID vertical heat pipe, with indication of sign conventions adopted here. Gravity acts downwards, in the direction of increasing z. Heat flux and steam flow are upwards and negative, while pressure gradient and liquid velocity are positive.

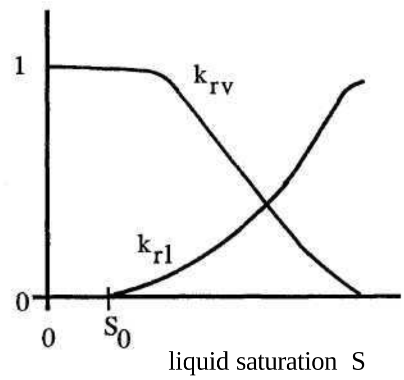

Figure 2. Typical shapes for the dependence of relative permeabilties on saturation. s_0 is a residual liquid saturation. The curves are generally taken to be monotonic and of opposite sense.

With the sign conventions indicated in Figure 1 the Darcy equations for the flow of vapour and liquid phases are

$$u_i = -\frac{k k_{ri}}{\nu_i}(\nabla p - \rho_i g), \; i = v, l, \qquad (3)$$

where ν_i is kinematic viscosity, k is permeability, k_{ri} is the relative permeability, ∇p is the pressure gradient, ρ_i is density and g is the gravitational constant. Subscripts v and l refer to vapour (or steam) and liquid phases respectively. The relative permeability functions k_{ri} depend on liquid saturation s reflecting experimental evidence that the effective permeability of a porous medium varies with the liquid saturation. The typical shapes of these functions are sketched in Figure 2.

When Equations 1, 2 and 3 are used to eliminate the pressure gradient term, the following relationship between p, s and Q is obtained (eg Pruess et al, 1986).

$$Q = \frac{[\varrho_l(p) - \varrho_v(p)]h_{vl}(p)}{\sigma_v(p,s) + \sigma_l(p,s)}, \qquad (4)$$

where

$$\sigma_i = 1/\lambda_i,$$

and

$$\lambda_i \equiv k k_{ri}/\nu_i, \quad i = v, l.$$

The relationship between p, s and Q expressed by Equation 4 is necessary for steady state conditions to hold in a vertical heat pipe. It defines a surface in p, s and Q space as in Figure 3. If p is fixed the curve in Figure 4 is typical. If Q is given Equation 4 defines curves in p, s space as in Figure 5.

These figures are obtained by numerically evaluating the thermodynamic variables ϱ, h and u, and by using linear relative permeabilities

$$k_{rl} = \begin{cases} 0, & 0 \le s \le 0.3 \\ 1 - (1-s)/0.7, & 0.3 < s \le 1 \end{cases} \qquad (5)$$

k_{rv} = [illegible]

Note that for some values of Q there is no real solution to Equation 4, and no steady heat pipe can give such a heat flux.

Then given Q a simulated steady heat pipe should have values of p and s that lie on or close to the line shown in Figure 5. In particular it is clear that if a steady state is to exist the values of p and s in the large constant element must lie on the appropriate curve (given Q). In general this has not been done in the simulations described previously (McGuinness and Pruess, 1987).

In fact if the large constant boundary is given values of p and s that lie on one of the steady state curves, simulations indicate that the heat pipe is *always* numerically stable. That is, whether it is liquid-dominated or vapour-dominated and no matter which end is held constant, the heat pipe is stable to changes in p and s, provided the fixed p and s boundary condition matches the given heat flux.

Numerical Steady States

Since the condition for steady state in Equation 4 relates p, s and Q, if the boundary condition of constant p and s does not satisfy Equation 4 for the given Q it is not expected that a steady state can be obtained. The surprising thing then is not that the heat pipe simulation as described in McGuinness and Pruess (1987) were sometimes unstable, but that they were sometimes *stable!* For in those simulations condition 4 for steady state was not satisfied by the constant element.

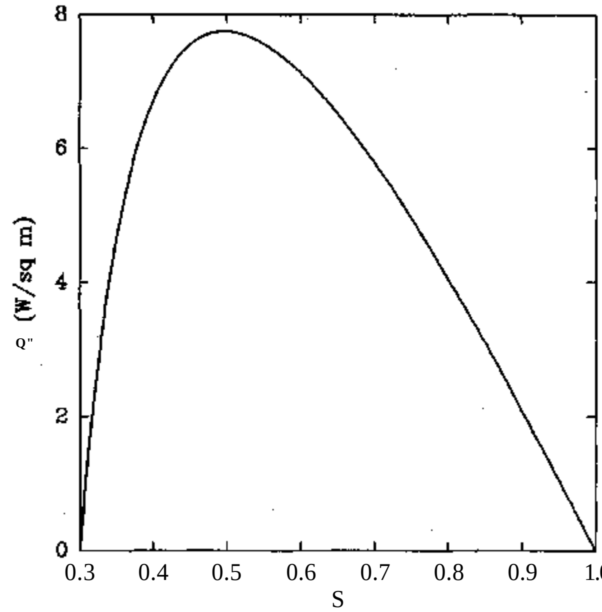

Figure 4. A slice through the surface in Figure 3 corresponding to holding p constant.

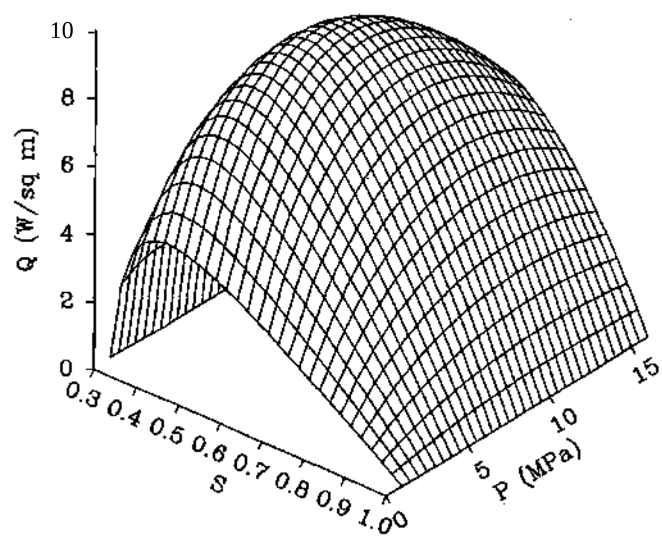

Figure 3. The surface in p, s and Q space defined by steady-state heat pipe conditions.

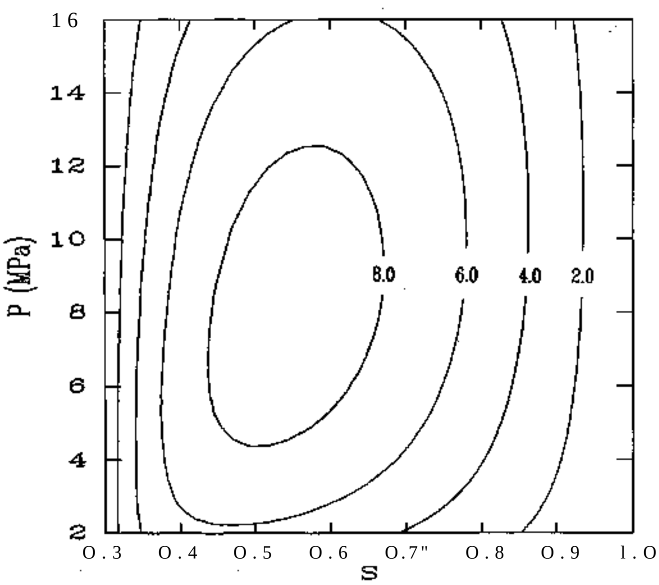

Figure 5. Contours of constant Q (W/m^2) for the surface in Figure 3.

The question then is, why does the numerical simulation sometimes approach a mathematical steady state? In particular, if the constant element is at the bottom of the heat pipe, why does the heat pipe simulation usually approach a vapour-dominated steady state?

The answer to this question lies in a consideration of the implications of upstream differencing of mobility terms in the simulation. The vital role played by the choice of differencing of mobilities has also been noted by Blakeley (1986) in the context of obtaining a condensate layer over a two-phase region. Blakeley has also independently reached conclusions similar to those in this paper (private communication).

Upstream differencing, or upwinding, is used in hyperbolic problems to stabilise computations. In MULKOM it is applied most crucially to the mobility; that is when the mobility of steam or liquid is to be evaluated at an interface, the net pressure gradient is checked to see in which direction that phase is flowing. The values of *p* and *s* in the upstream element are used to evaluate mobility, rather than using an average value of *p* and 5.

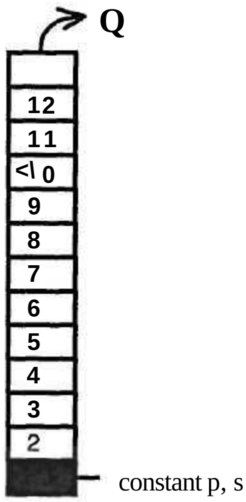

Figure 6. Numbering conventions used in the text when referring to numerical techniques applied to a heat pipe.

A2DMAP

To see the effect of upwinding on heat pipe simulations we concentrate here on the configuration in Figure 6 with the constant *p* and *s* boundary condition at the bottom. Then labelling the bottom element number 1 and noting that steam goes up while liquid falls down the steady state conditions are

$$u \quad = \quad -u_v \ = \ \backslash_{vi}(Vp \ - \ g_v g) \qquad (6)$$
$$u \ = \ u, \ = \ -A_{/2}(V> - \ gig) \qquad (7)$$

where $\backslash_{vl}$ means vapour mobility evaluated at the upstream (constant) element number 1, and Aj_2 means liquid mobility evaluated at the upstream element number 2, and

$$\begin{aligned} Avi &= X_v(pi, \ 5i), \\ A/_2 &= A/(p_2, \ s_2), \ \text{etc.} \end{aligned} \qquad \textbf{(8)}$$

and $u \ = \ —Q/h_v i$ as before.

Densities may also be upstream differenced with little effect on the arguments here. In general *Vp* and *g* depend on both p_x and p_2. Equations 6 and 7 may be viewed as a 2-dimensional map taking us from the fixed *(pi,* si) values at the boundary element to the values of (p_2, 52) at the next computation element. Equation 6 may be used first to find p_2, given *pi* and si and *Q* (or *it).* Equation 7 may then be used to find s_2 given p_2, pi and *Q*. This process may be continued up the heat pipe to get $(p_3, \ s_3)$, $(p_4, \ 54)$... If there is a physical solution at each step it is unique and the map is invertible.

If *Vp* is eliminated from Equation 6 and 7 we obtain the analogue of Equation 4.

$$Q = \frac{(\varrho_l - \varrho_v)h_{vl}}{\sigma_{v1} + \sigma_{l2}} \qquad (9)$$

If *Q*, pi and si are given, Equation 9 relates p_2 and s_2. That is, Equation 9 describes a *line* in *p* and *s* space on which p_2 and s_2 must lie for steady state. Repeated applications of the map may be regarded as generating many lines. These lines do not cross since the map is invertible.

The steady state curves described by Equation 4 are invariant curves under the above mapping — a point *(pi, s\)* on such a curve is mapped onto the same curve by Equation 9. If the pressure range is appropriately restricted Figure 5 shows that there are two invariant lines, which join up to form a closed loop if the pressure range is expanded. The question raised above then becomes a question of whether the 2-dimensional mapping approaches one (or both) of these invariant lines.

It is clear that Equation 6 in this context imposes a strictly decreasing pressure sequence *pi, p_2, Ps,--.* when applied repeatedly. Assuming this sequence stays inside the appropriate pressure range it is possible to ignore (or collapse out) the pressure dimension and consider only the saturation dimension. Then Equation 9 becomes a 1-dimensional map, mapping sj to s_2, which may be applied repeatedly to obtain s_n in general. Equation 4 is then an equation describing the fixed points s^* of this map. There are only 2 such fixed points; one vapour-dominated, one liquid-dominated. The local stability of these fixed points gives the global behaviour of this 1-dimensional map.

The 1-dimensional map may be written implicitly as

$$\sigma_{l\ n+1} \ = \ (\varrho_l - \varrho_v)h_{vl}/Q - \sigma_{vn}, \ n = 1, 2, \ldots \qquad (10)$$

where

$$\sigma_{in} \ \equiv \ \frac{\nu_i}{k k_{ri}(s_n)}, i = v, l.$$

The fixed points are when $s_n \longrightarrow s^*, n \rightarrow 00$ and

$$a\backslash \ \equiv \ (7i(s^*) \ = \ (g, \ - \ g_v)h_v/Q \ - \ <rl, \qquad (11)$$

for which figures 3, 4 and 5 clearly show there are two solutions

$$s^* = s^l{*} \text{ or } s^v{*} \qquad (12)$$

when *p* and *Q* are in appropriate ranges. One solution (s^v*) corresponds to a vapour-dominated heat pipe, and the other (s^1*) to a liquid-dominated heat pipe. Expanding Equation 10 about the fixed points shows that the local stability of these two fixed points is dependent on the criterion

$$\frac{Ki(s)}{k_{rv}(s)} \ < \ \sqrt{\frac{\beta \nu_l}{\nu_v}}, \qquad (13)$$

where

$$\boldsymbol{P} \ = \ \left| \frac{\partial k_T i}{\partial s}, \frac{dk_{rv}}{\partial s} \right|$$

and all quantities are evaluated at the fixed point under consideration. When this criterion is satisfied the fixed point is stable.

Noting the general shape of the relative permeability curves sketched in Figure 2, and that typically one phase has a very small relative permeability compared to the other, it is clear that in general s^v* is stable and s^l* is unstable.

In fact, stability switches when the inequality in Equation 13 is replaced by equality. The resulting equation is in fact the equation for the maximum point of the steady-state curve in Figure 4, if p is held constant. That is, with the current configuration, s^v* is always stable, and 5* is always unstable. As Q is increased (at given p), s^v* becomes less strongly stable, and approaches the unstable fixed point s^l* (see Figure 8), to coalesce at the moment of stability switch, when there is no distinguishing between a vapour-dominated and a liquid-dominated heat pipe.

Since the map is 1-dimensional and these are the only fixed points the following global stability comments hold.

If the starting point is $s_0 < s_t < s^l*$ the map will take s quite rapidly to s^v* and a stable vapour-dominated heat pipe results. If $si = s^l*$ the map will not change s and a stable liquid-dominated heat pipe results, since the boundary conditions have been placed right on the steady state curve in Figure 5. If $S\text{-}L > s^1*$, s will increase under the map until single-phase liquid conditions hold and no two-phase steady state will be achieved. Figure 7 illustrates this stability behaviour.

These observations based on the behaviour of the 1-dimensional map in Equation 10, are consistent with full numerical simulations using MULKOM.

The same arguments go through for the other configuration with the constant element at the top of the computation grid. Then the indices v and / are reversed, and the stability picture for the 1-dimensional map is reversed with the liquid-dominated heat pipe being the stable fixed point.

CONCLUSIONS

The main conclusion of this paper is that the numerical stability behaviour observed for heat pipes is a direct consequence of upstream differencing of mobilities. While the mathematical conditions for a steady state heat pipe are quite restrictive, requiring the constant p and s boundary conditions to match up with the imposed heat flux Q, upstream differencing allows a steady state simulated heat pipe for a wide range of pressure and saturation boundary conditions (given Q). This simulated heat pipe asymptotes towards either the liquid-dominated or vapour-dominated (mathematical) steady heat pipe, depending on boundary conditions.

It is tempting to speculate on the physical implications of this work. Upstream differencing may have some physical basis, in that the mobility of a phase across an interface should perhaps intuitively depend on saturation in the region it is coming from, rather than in the region it is going to. If this is the case, the comments made in a previous paper (McGuinness and Pruess, 1987) still hold, that a vapour-dominated geothermal reservoir would be expected to develop if there is pressure and saturation control at depth, and that a liquid-dominated geothermal reservoir would be expected to develop if there is pressure and saturation control near the top of the reservoir.

ACKNOWLEDGEMENTS

This work would not have started without the insight and experience brought to it by Karsten Pruess. The crucial parts of this paper were the direct results of discussions with John Burnell and Margaret Blakeley. Thanks also to Graham Weir, Steve White, Warwick Kissling and Roger Young for helpful discussions.

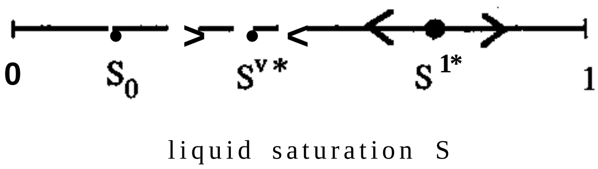

Figure 7. A stability diagram for the steady-state fixed points s^v*, s^l*. The arrows show in which direction an initial point s will move when iterated upon using the ID map referred to in the text.

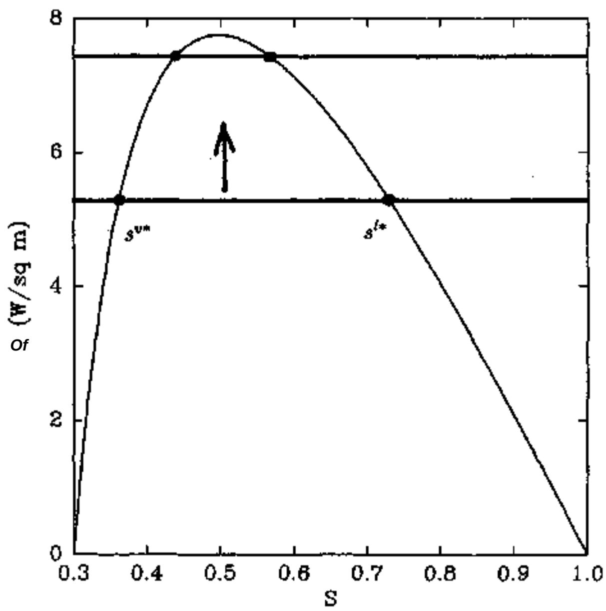

Figure 8. The steady-state fixed points on the same plot as Figure 4, showing that as Q increases (at suitable given p), the fixed points coalesce.

REFERENCES

Blakeley M. (1986) *Geothermal Reservoir Modelling,* Ph.d. thesis, Dept. of Theoretical and Applied Mathematics, Auckland University, April 1986.

McGuinness M.J. and Pruess K (1987) *Unstable heat pipes,* in the proceedings of the Ninth New Zealand Geothermal Workshop, Auckland University, November 1987, pp.147-151.

Pruess K (1983) *Development of the general purpose simulator MULKOM,* Annual Report 1982, Earth Sciences Division, Report LBL-15500, Lawrence Berkeley Laboratory.

Pruess K. (1985) *A quantitative model of geothermal reservoirs as heat pipes in fractured porous rock,* Transactions of 1985 Symposium on Geothermal Energy, Geothermal Resources Council 1985 Annual Meeting, Volume 9 — Part II, pages 353-362.

Pruess K, Celati R., Calore C, Cappetti G. (1986) *On fluid and heat transfer in deep zones of vapor-dominated geothermal reservoirs,* Report LBL-22810, Earth Sciences Division, Lawrence Berkeley Laboratory.

Straus J. M., Schubert G. (1981) *One-dimensional model of vapor-dominated geothermal systems,* J. Geophys. Res. 86 (1981) 9433-9438.

Truesdell A. H., White D. E. (1973) *Production of superheated steam from vapor-dominated geothermal reservoirs,* Geothermics 2 (1973) 154-173.

White D. E., Muffler J. P., Truesdell A. H. (1971) *Vapour-dominated hydrothermal systems compared with hot-water systems,* Economic Geology 66 (1971) 75-97.